Direct imaging of dopant distributions in silicon by scanning transmission electron microscopy

S. J. Pennycook and J. Narayan
Solid State Division, Oak Ridge National Laboratory, Oak Ridge, Tennessee 37831

(Received 9 April 1984; accepted for publication 30 May 1984)

The first direct images of dopant distributions in Si have been observed using scanning transmission electron microscopy, by detecting Rutherford-scattered transmitted electrons. Strong atomic number (Z) contrast is obtained allowing images to be formed of Bi at concentrations of the order of 0.2 to 1 at. % and of Sb at concentratiosn of 0.5 to 6 at. %. The image contrast from cross-section specimens correlated closely with the dopant concentration profiles determined by x-ray microanalysis and with Rutherford ion backscattering analysis of the bulk materials. This technique should prove extremely valuable for studying dopant segregation phenomena in semiconductors.

Conventional transmission electron microscopy (TEM) relies on diffraction or phase contrast mechanisms to form the image and can, therefore, only image the dopant in semiconductors when it forms a separate distinct phase, such as a precipitate. With scanning transmission electron microscopy (STEM), incoherent imaging modes are available which allow the formation of images showing strong atomic number (Z) contrast. The image intensity simply reflects the number of atoms under the beam, and it is not critical whether the atoms are isolated or in precipitate form. We have directly imaged Bi concentrations of 0.2 to 1 at. % and Sb concentrations of 0.6 to 6 at. % in ion implanted silicon using cross-section samples. These results represent the first direct images of dopant distributions in semiconductors by electron microscopy.

The Z-contrast image is obtained in STEM with an annular detector placed around the transmitted beam (Fig. 1). By collecting scattered electrons over a wide angular range, we achieve a very efficient imaging mode that gives strong Z contrast.[1–4] The ratio of the annular detector signal to the energy loss intensity can be used to suppress contrast due to thickness variations. With crystalline materials, however, strong diffraction contrast effects are obtained, similar to tilted dark field TEM. While diffraction contrast is valuable for imaging structural defects that introduce large cumulative lattice distortions, it may obscure any Z contrast in the image. To avoid diffraction effects the detector can be arranged to collect only those electrons scattered to large angles (Fig. 1).[5,6] Here the dominant scattering mechanism is Rutherford so that the image intensity is proportional to $\Sigma n_i Z_i^2$, where n_i is the number of atoms of element i under the electron probe. In this letter, we show that Bi concentrations around 0.5 at. % or Sb concentrations around 2% exhibit strong Z contrast. In ion implanted samples, dopant profiles are determined and the results are compared with those obtained using x-ray microanalysis and Rutherford ion backscattering (RBS) techniques. Small variations in dopant concentrations are detected, indicating the usefulness of the STEM technique in studying dopant segregation phenomena in semiconductors.

Samples were prepared by ion implantation followed by solid-phase-epitaxial growth, to produce supersaturated alloys having dopant concentrations high enough for direct imaging. The (100) Si samples were implanted with $^{209}Bi^+$ (250 keV, 5×10^{15} cm^{-2}) at room temperature, and annealed at 550 °C for 40 min. under flowing dry N_2 gas. The solid-phase-epitaxial (SPE) growth occurred to within 70 nm of the surface,[7] followed by a 40 nm region containing dislocations and twins and a 30 nm polycrystalline region. A Si–Sb alloy was prepared by implanting $^{121}Sb^+$ (80 keV, 1.35×10^{16} cm^{-2}) at liquid nitrogen temperature into (100) Si. On furnace annealing at 550 °C for 40 min, SPE growth occurred to within 30 nm of the surface, the remaining material being polycrystalline with some twins. Cross-section samples were prepared using an ion-beam thinning procedure and studied in a Philips EM-400 TEM/STEM. Companion specimens were analyzed by Rutherford backscattering and ion channeling techniques.

The conventional TEM image of the Bi implanted sample [Fig. 2(a)] shows a band of dislocation loops underlying the SPE-grown region, and the layers of twinned and polycrystalline Si near the surface containing a few Bi precipitates. The image is dominated by diffraction contrast. Figure 2(b) shows an annular dark field STEM micrograph of the same region, using the same diffraction conditions. The image resolution is considerably poorer than the TEM image, since we have no field emission gun, but the same diffraction contrast mechanisms are operating. To form an image using

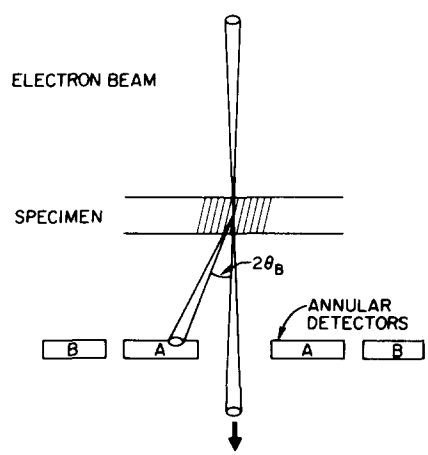

FIG. 1. Annular detector arrangement in STEM; A detects diffracted electrons, while B detects primarily Rutherford-scattered electrons.

 © 1984 American Institute of Physics

Downloaded 04 Jun 2004 to 160.91.48.238. Redistribution subject to AIP license or copyright, see http://apl.aip.org/apl/copyright.jsp

FIG. 2. Cross-section electron micrographs of $^{209}Bi^+$ (250 keV, 5×10^{15} cm^{-2}) implanted Si (100) SPE grown at 550 °C/40 min. (a) Conventional TEM image, (b) STEM image of the same region using diffraction contrast, (c) STEM image using high-angle detector showing bright stripe due to Bi.

electrons scattered to high angles (65–150 mrad), the microscope camera length was reduced considerably. It was found that residual diffraction contrast effects remained, due to high order reflections of the {220} systematic set. By orienting the sample to avoid strong low-order reflections, we obtained the image shown in Fig. 2(c). The stripe parallel to the

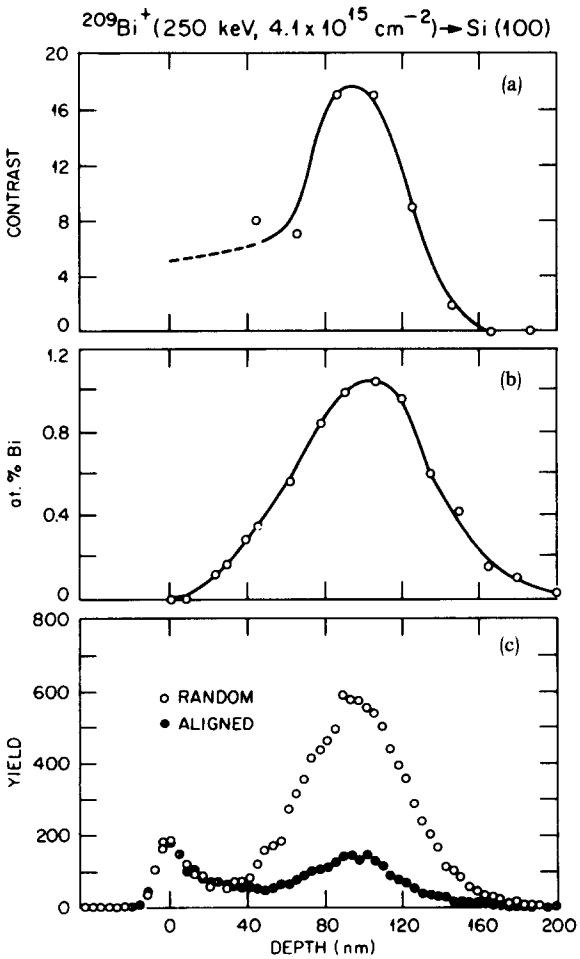

FIG. 3. (a) Intensity profile of high-angle detector contrast; variable results were obtained near the surface (broken line) due to precipitates, (b) x-ray profile of Bi concentration, (c) bulk RBS spectrum from Bi.

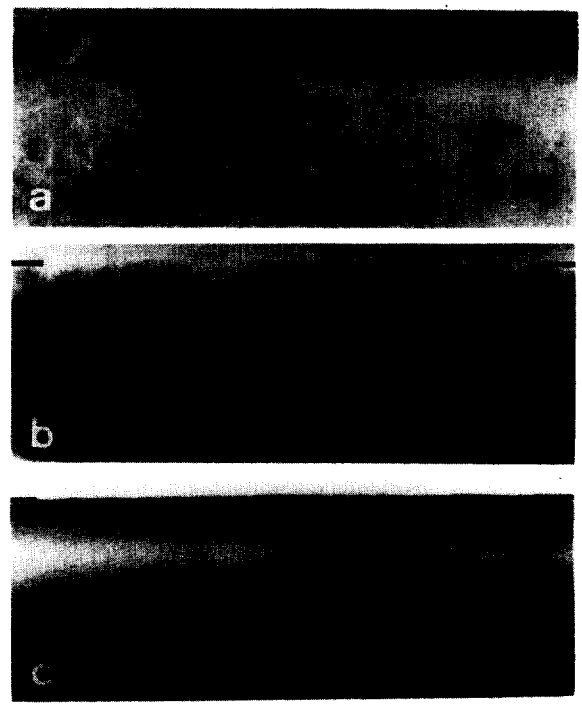

FIG. 4. Cross-section micrographs of $^{121}Sb^+$ (80 keV, 1.35×10^{16} cm^{-2}) implanted Si (100) SPE grown at 550 °C/40 min, (a) TEM, (b) STEM image using diffraction contrast, (c) STEM image from Rutherford scattered electrons showing Sb distribution. Markers indicate original sample surface.

sample surface is due to Bi incorporated into the Si lattice and reflects the Gaussian implantation profile. No diffraction contrast effects are observed and considerably more precipitates are visible than in Figs. 2(a) or 2(b). However, the image is noisier than in Fig. 2(b) since only a small fraction of the transmitted electrons are scattered to high angles. Faint striations are visible in all images which are due to thickness variations. These could be removed from Fig. 2(c) by ratioing the annular detector signal with the energy loss intensity,[1] but one would then be limited to specimens less than 50 nm in thickness, whereas one of the advantages of high angle imaging is its effective penetration of thick samples.[8]

A profile of the Bi concentration has been taken by detecting the x-ray fluorescence [Fig. 3(b)] and is compared to the high-angle intensity profile after subtracting the uniform background of the Si matrix [Fig. 3(a)]. The x-ray profile is somewhat broader, since a thicker region of sample was used to obtain sufficient intensity, which resulted in broadening of the electron probe. Clearly, however, the image contrast reflects the Bi concentration. Also shown is the RBS analysis from a bulk sample [Fig. 3(c)] giving a profile in agreement with the microscopic results. The ⟨110⟩ aligned RBS data allow the substitutional fraction of Bi to be determined as a function of depth. Electron channeling analysis can also determine substitutional fractions of dopants microscopically.[9] To perform the analysis at each point in Fig. 3(b) would require a small collimated electron probe which can only be obtained from a field emission gun. We have analyzed a region of 60 nm diameters centered on the peak in the Bi profile and found it to be 76% substitutional, in agreement with the value of 80% determined by RBS.

Figure 4 shows the results from the Sb implanted sample. Since Sb has a lower atomic number than Bi, corre-

Downloaded 04 Jun 2004 to 160.91.48.238. Redistribution subject to AIP license or copyright, see http://apl.aip.org/apl/copyright.jsp

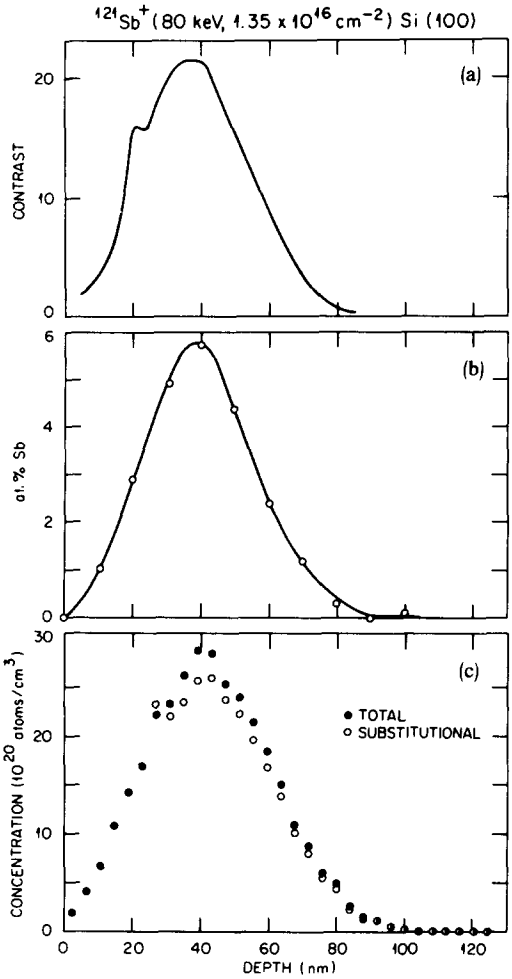

FIG. 5. (a) High angle detector contrast, (b) Sb profile determined by x-ray microanalysis, (c) RBS analysis of Sb.

spondingly higher concentrations are required for direct imaging. The diffraction contrast images taken in TEM [Fig. 4(a)] and STEM [Fig. 4(b)] both show the polycrystalline layer. Figure 4(c) shows the image obtained using Rutherford scattered electrons, which clearly delineates the implantation profile of Sb, and shows that no Sb precipitates have formed. The narrow line visible in the image probably indicates segregation of Sb at the boundary of the single crystal and polycrystalline regions. The STEM images are of better quality than Fig. 2 since a high brightness LaB_6 gun was used. This allowed the x-ray profile [Fig. 5(b)] to be taken from the same region as used for imaging, and good correlation was seen with the image contrast [Fig. 5(a)]. Contamination problems did not allow enough points to be taken in the x-ray profile to reveal the shoulder seen in the image contrast. The high angle image has much greater sensitivity for detecting segregation phenomena. The microscopically determined Sb profile is also in agreement with the bulk RBS analysis [Fig. 5(b)]. Electron channeling analysis using a 35-nm-diam probe on the peak of the Sb profile indicated 72% substitutionality compared to a value of 89% determined by RBS. This is probably due to some of the polycrystalline layer being included in the analyzed volume.

It is clear from these results that the contrast in an image formed from Rutherford scattered electrons accurately reflects the dopant concentration, provided care is taken to avoid residual diffraction contrast effects. It should be possible to use such an image for elemental mapping at high spatial resolution in thin specimens. The characteristic x-ray emission cannot be used for this purpose since the intensity emitted by the dopant is too low when using a small probe. The image obtained with a high angle annular detector offers an alternative, and it should be possible to accurately calibrate the image by taking a few sample x-ray analyses from representative points.

In conclusion, we have shown that heavy dopants in silicon can be directly imaged using Rutherford scattered transmitted electrons. Image contrast from Bi (0.2 to 1 at. %) and Sb (0.6 to 6 at. %) was directly correlated with the dopant concentration determined by x-ray microanalysis, and with Rutherford backscattering and ion channeling analysis from bulk material. Such images will be of great value in studying dopant segregation effects at twins and dislocations particularly when the dopants cluster or form precipitates that are below the resolution limit of the diffraction contrast imaging mode.

The authors would like to thank O. W Holland for research collaborations. This research was sponsored by the Division of Materials Sciences, U. S. Department of Energy under contract DE-AC05-840R21400 with Martin Marietta Energy Systems, Inc.

[1]A. V. Crewe, J. P. Langmore, and M. S. Isaacson, in *Physical Aspects of Electron Microscopy and Microbeam Analysis*, edited by B. M. Siegel and D. R. Beaman (Wiley, New York, 1975), p. 47.
[2]M. M. J. Treacy, A. Howie, and C. J. Wilson, Philos Mag. A **38**, 569 (1978).
[3]C. Mory, C. Colliex, B. Revet, and E. Delain, Ultramicroscopy **7**, 161 (1981).
[4]S. J. Pennycook, Contemp. Phys. **23**, 371 (1982).
[5]M. M. J. Treacy, J. Microsc. Spectrosc. Electr. **7**, 511 (1982).
[6]S. J. Pennycook, A. Howie, M. D. Shannon, and R. Whyman, J. Mol. Catalysis **20**, 345 (1983).
[7]J. Narayan, O. W. Holland, and B. R. Appleton, J. Vac. Sci. Technol. B **1**, 871 (1982).
[8]S J. Pennycook and D. McMullan, Ultramicroscopy **11**, 315 (1983).
[9]S J. Pennycook, J. Narayan, and O. W. Holland, Appl. Phys. Lett. **44**, 547 (1984).

Downloaded 04 Jun 2004 to 160.91.48.238. Redistribution subject to AIP license or copyright, see http://apl.aip.org/apl/copyright.jsp